24th INTERNATIONAL CONGRESS ON SOUND AND VIBRATION
23–27 July 2017, London

NUMERICAL SIMULATION OF ONE-STAGE GEARBOX DYNAMICS IN THE PRESENCE OF SIMULTANEOUS TOOTH CRACKS

Ahmed Mohamed, Sadok Sassi and Mohammad Roshun Paurobally

Qatar University, College of Engineering, Doha, Qatar
email: a.mohamed@qu.edu.qa

Gears are vital components in various industrial machinery. Tooth fatigue crack is amongst the most common causes of gear failure. Early detection of tooth cracks is crucial for effective condition-based monitoring. This study aims at investigating the dynamics of a one-stage spur gearbox, having multiple tooth cracks located simultaneously on the pinion and the gear. The numerical simulation of the vibration behaviour is obtained using a 6 DOF dynamic model, that takes into account the lateral and the torsional motions of the two gears of the gearset. The effect of inter-tooth friction was taken into consideration in this study. The time-varying mesh stiffness was evaluated using the finite element method, while the vibration response is obtained using a developed MATLAB code. Different vibration signal features were applied on the time and frequency domains of the residual signals, to examine their sensitivity. The hunting tooth phenomenon, where a cracked tooth on the pinion gets in contact with a cracked tooth on the gear, was particularly investigated. To make the analysis more realistic, different scenarios of various depths and number of cracks were considered. For each one of these scenarios, the use of statistical signal features showed contradictory patterns and the use of such features could be deceptive if not considered properly. This study has the potential to improve the early detection of simultaneous gear tooth cracks.
Keywords: spur gear, simultaneous tooth cracks, hunting tooth, numerical simulation, vibration analysis

1. Introduction

Gear tooth cracks can occur due to excessive loads, operation under improper conditions or installation problems. The presence of cracks alters the gear mesh stiffness (GMS) and consequently the vibration response of the system [1]. The crack propagation scenario of the same depth distribution throughout the whole gear width is usually considered assuming a uniform load distribution. Finite element method (FEM) is the most popular technique used for GMS evaluation [2]. Vibration health monitoring is one of the common techniques that can be used to effectively detect gear tooth cracks. Early fault detection allows optimally scheduled maintenance to prevent sudden failure and therefore higher cost savings [3]. During the past few years, dynamic modeling and simulation have become a good alternative to the experimental method for studying the dynamic behaviour of a gear system and are still the subject of much ongoing research. Different gear dynamic models have been developed and applied for the dynamic response simulation [4]. A six-DOF gear dynamic model which considered inter-tooth friction was conceived in [5]. A great deal of research has been focusing on faulty pinion only without considering faulty gears in a gearset. Time-domain and frequency-domain analysis are widely applied signal processing techniques for gear tooth fault detection. Time domain statistical indicators such as kurtosis (KU), root mean square (RMS), and crest factor (CF) are usually applied to the residual vibration signal to monitor the crack propagation [6].

The main objective of this work is to bring more insights into more realistic cases where multiple cracks exist simultaneously in different locations and to different extents present on both the pinion and gear, using numerical simulation and dynamic modeling done by MATLAB software.

2. GMS modelling with simultaneous tooth cracks

In this study, the crack path is assumed to start at the top of the root fillet and changes its direction after reaching the centre line of the tooth. Then, it propagates towards the top of the root fillet on the other side, moving in straight lines with a crack propagation angle of 20^o, as presented in [1]. Supposing that *CD* is the Crack Depth and *PD* is the total crack Path Depth shown as a red dashed line in Fig. 1, the Crack Depth Percentage (*CDP*) can be obtained as:

$$CDP = \frac{CD}{PD} \text{ x } 100 \tag{1}$$

The parameters used in the modelling are given in Table 1 [7]. The backup ratio was taken as 3.3 to avoid the rim thickness effect on the tooth deflection, and the fillet curves were assumed to be circular.

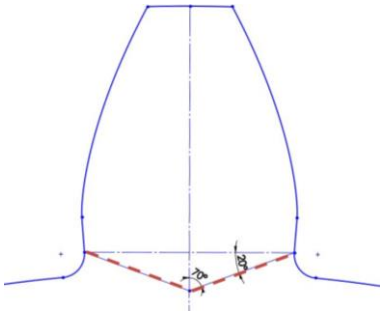

Figure 1: Crack propagation path.

Table 1: Gear parameters used [7].

Parameter	Pinion	Gear
Number of teeth	25	30
Pressure angle (degree)	20	
Face width (mm)	20	
Module (mm)	2	
Elastic modulus (N/m^2)	2×10^{11}	
Poisson's ratio	0.3	
Contact ratio	1.63	
Crack propagation angle (degrees)	20	
Fillet radius (mm)	0.4	
Crack width (mm)	20	
Total depth of the crack path (mm)	3.8	

The individual tooth stiffness for both the pinion and the gear was evaluated using FEM. A finite element simulation was done using SolidWorks software. Figure 2 illustrates how the stiffness of a single tooth is calculated. A force is applied normal to one side of the tooth, acting along the line of action while the bore was fixed. From the simulation results, the deflections δ_x and δ_y can be used to get δ in the direction of the force, which was adopted by [6]. As the stiffness varies with respect to the angle θ between the start of the involute curve and the location at which the force is applied, different positions were studied one at a time. At each location, the deflection of the tooth is recorded (δ_i) in the same direction of the force and was used to calculate the tooth stiffness as $K_i = F/\delta_i$.

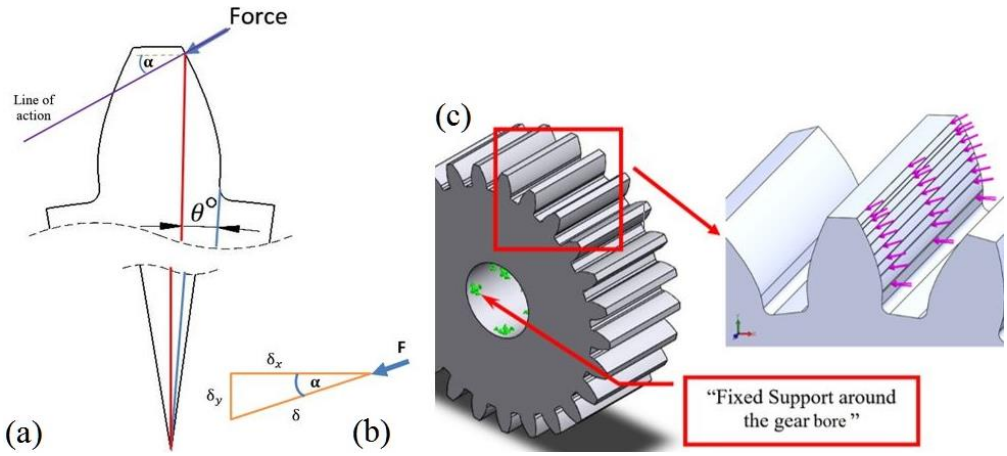

Figure 2: (a) Transmitted force normal to the tooth face. (b) Resolving the displacement components. (c) Boundary conditions applied

In Fig. 3, the overall mesh of the pinion is displayed. A finer mesh was used at the location where the force was applied and at the crack region as well. The effect of the Hertzian contact (K_h) was taken into account as a constant value calculated by the formula presented in [6,7].

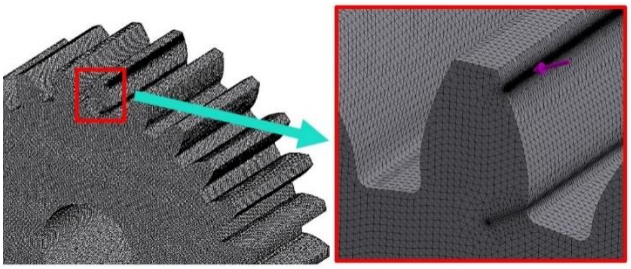

Figure 3: Overall meshing of the pinion and mesh control at the force applied area, and the crack region.

During the meshing between two mating gears, the contact can be single (between two teeth) or double (between two pairs or four teeth). Therefore, the total gear mesh stiffness will vary and can be calculated as follows:

For one pair in contact:

$$K_t = \frac{1}{\frac{1}{k_{p1}} + \frac{1}{k_h} + \frac{1}{k_{g1}}}. \quad (2)$$

For two pairs in contact:

$$K_t = \frac{1}{\frac{1}{k_{p1}} + \frac{1}{k_h} + \frac{1}{k_{g1}}} + \frac{1}{\frac{1}{k_{p2}} + \frac{1}{k_h} + \frac{1}{k_{g2}}}. \quad (3)$$

Although the pinion is more susceptible to gear tooth cracks, sometimes cracks appear on the gear as well. Figure 4 illustrates the difference in the GMS when a crack is present on the pinion, the gear, and both gears that mate while meshing. For the case of healthy teeth in contact, the graph in Fig. 4 shows the alternation of one pair in contact (low stiffness) and two pairs (high stiffness). The GMS is the lowest in the case of coincident cracks.

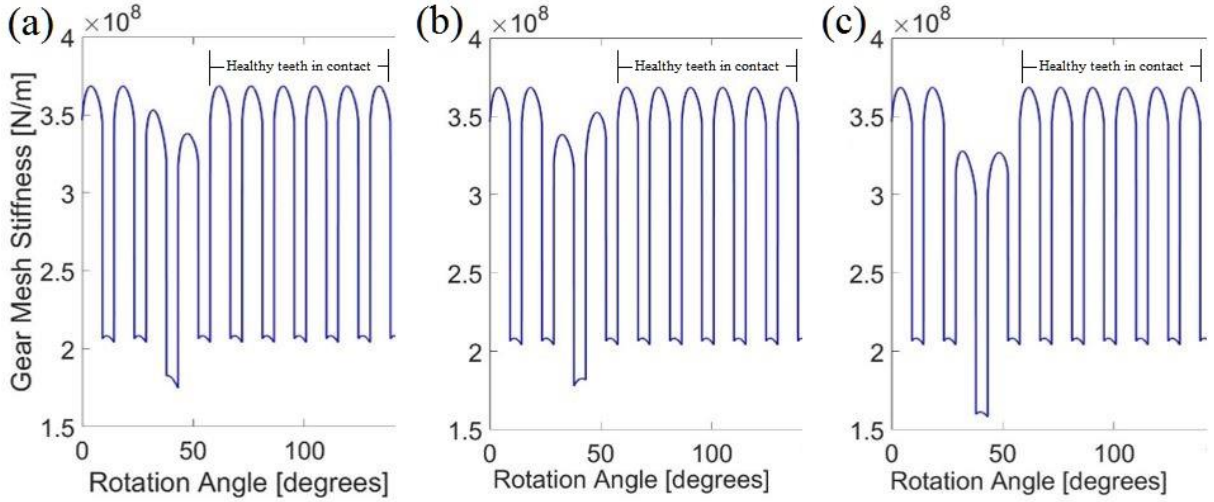

Figure 4: Faulty gears GMS; (a) Crack on the pinion with 25% CDP; (b) Crack on the gear with 25% CDP; (c) Cracks mate with each other with 25% CDP

2.1 Proposed Multiple Cracks Scenarios

Two main scenarios are proposed to study the possibility of having multiple cracks located on both the pinion and the gear. The first one is the case where the cracks do not coincide with each other, while the other scenario is when they coincide, taking into consideration different CDP and number of cracks. The data of the 12 cases studied are summarized in Table 2.

Table 2: Data for the studied cases

No. of cracks	CDP (%)	Coincide	Case
1	15	No	1
		Yes	2
	25	No	3
		Yes	4
3	15	No	5
		Yes	6
	25	No	7
		Yes	8
6	15	No	9
		Yes	10
	25	No	11
		Yes	12

3. Gearbox dynamic modelling

Using the lumped mass model, the effect of simultaneous tooth cracks on the vibration response can be extracted. A six DOF model has been used as it is the simplest model that can accommodate the effect of friction caused by the sliding of the mating teeth. Moreover, the six DOF model is more responsive to gear tooth cracks than higher DOF models [8]. The dynamic model used in this study is shown in Fig. 5, which was adopted in [1,5]. The GMS (K_T) is taken along the *y*-axis, thus the friction will be along the *x*-axis. The parameters used in this dynamic model are adopted from [5] and are given in Table 3. The radial stiffness and damping of the bearings are assumed to be the same both horizontally and vertically, and they have the same values for the pinion and gear. The friction coefficient was taken to be 0.06 [5], that varies with respect to the rotational angle between -0.06 and 0.06. The load sharing ratio (LSR) is an important factor for finding the friction force. In the case of double tooth contact, the contact force is not distributed equally among the teeth [9]. The LSR for an individual pair can be calculated as:

$$LSR_i = \frac{K_{t_i}}{K_{t_1} + K_{t_2}}. \tag{4}$$

where i represents the number of tooth pairs concerned.

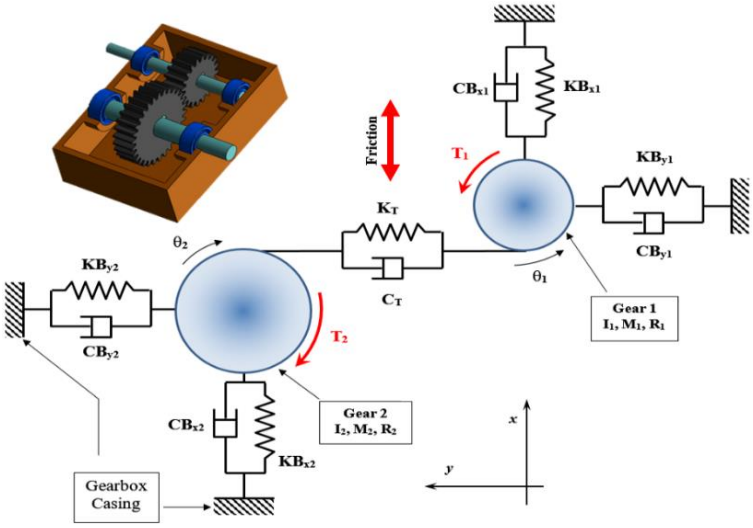

Figure 5: One-stage six-DOF gearbox dynamic model.

Table 3: Parameters of the gear system used in the dynamic model [5].

Parameter	Pinion	Gear
Base radius of the pinion and gear (mm)	23.49	28.20
Mass of the pinion and gear (kg)	0.3083	0.4439
Mass moment of inertia of pinion and gear (kg m^2)	9.633×10^{-5}	1.998×10^{-4}
Applied torque (N m)	50	60
Input shaft frequency (Hz)	40	
Radial stiffness of the bearings (N/m)	6.56×10^8	
Damping coefficient of the bearings (N s/m)	1.8×10^3	
Total damping between meshing teeth (N s/m)	67	

In this work, the friction force is considered to be an external force where all the dynamic effects of the normal force are excluded. In fact, the magnitude of the friction force depends on the dynamic friction coefficient (μ) and the contact force (F_c) between the teeth along the line of action. The frictional force (F_f), is calculated as $F_f = \mu F_c$. However, the transmitted and contact forces should be determined first. The transmitted force (F_T) caused by the applied torque (T) can be calculated knowing the pitch radius (R_p) of the gears as $F_T = T/R_p$.

Therefore, the contact force (F_c) along the line of action will be constant and can be obtained as:

$$\boldsymbol{F_c} = \frac{\boldsymbol{F_T}}{\boldsymbol{cos}(\Phi)}. \tag{5}$$

where Φ is the pressure angle.

The friction force can be calculated as:

$$\boldsymbol{F_f} = \boldsymbol{\mu} \cdot \boldsymbol{LSR} \cdot \boldsymbol{F_c}. \tag{6}$$

where *LSR* in a single contact case is equal to unity.

The friction force applied to the gear will be the same magnitude as that applied to the pinion at the same contact points, but in the opposite direction. The friction forces will also exert moments on the gears. These moments can be calculated by first identifying the moment arms, taking the contact geometry of the gear teeth into consideration (Fig. 6). The Cartesian coordinates of the contact points G and H are already known from the contact analysis. Also, points O_1 and O_2 are known, so both $\overline{O_1F}$ and $\overline{O_2I}$ can be calculated, and thus the frictional moment arms ($\overline{FG}$ and $\overline{FH}$ for the pinion, and $\overline{IH}$ and $\overline{IG}$ for the gear) can be identified. Then, the angles φ_1, φ_2, φ_3, and φ_4 are calculated using the dot product of two Euclidean vectors. Finally, the frictional moments are obtained by multiplying the friction force at the contact points with their respective arms. More details can be found in [10].

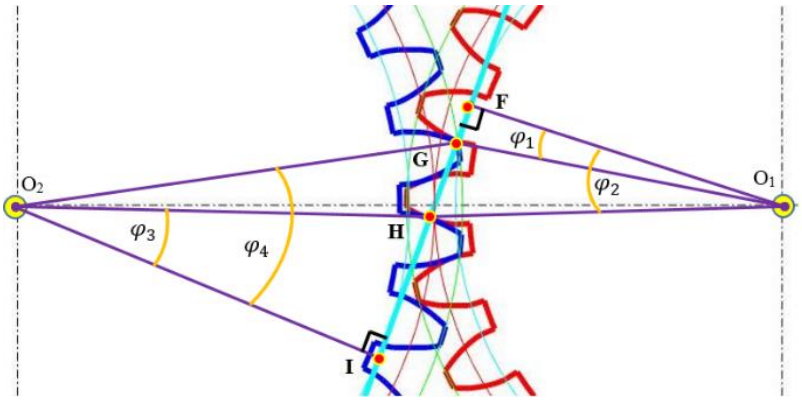

Figure 6. Contact geometry for frictional moment analysis.

4. Vibration response in the time-domain

The ODE4 function in Simulink was used for modelling the system equations of motion, and to get the same vibration response signal length with a fixed time step. A normally distributed noise was added with a Signal-to-noise ratio value of 20 dB to include the measurement noise influence. One simulated revolution for the pinion was considered, where the first revolution including the transient response, was excluded. The sampling frequency of 400 kHz was used to prevent aliasing and get better resolution. The y-displacement of the pinion was analysed for all the studied cases. Then, the residual signal was obtained by subtracting the time-domain healthy signal from the signal with faults

to ensure that the remaining signal is only related to the faults. Samples of the residual signals for case 7 and 8 are shown in Fig. 7.

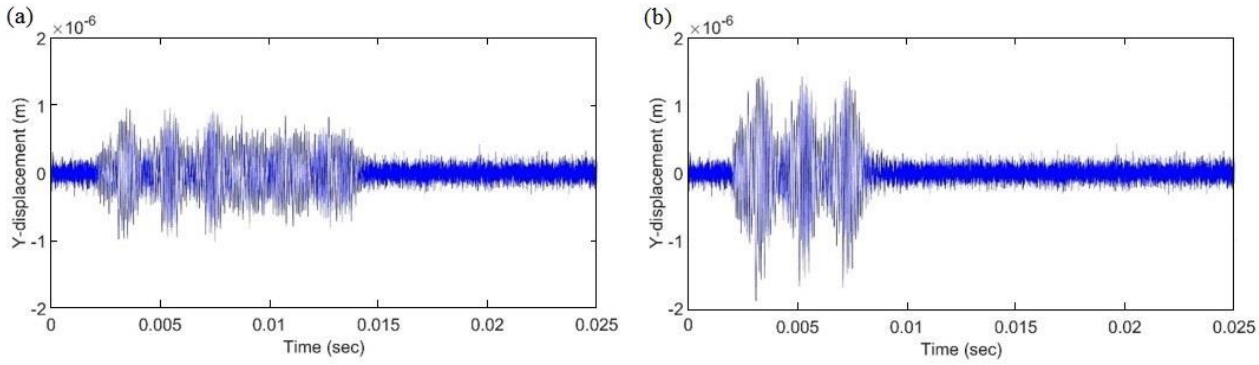

Figure 7: Residual signal; (a) Case 7. (b) Case 8.

4.1 Time domain statistical indicators

Taking the values of healthy gears case as a reference, the percentage change of the indicators was calculated. Figure 8 shows the effect of the studied cases on the RMS, KU, and CF. It is clear that the value of the RMS increases with the increase in the number of cracks, the CDP, and when the cracks coincide. On the other hand, the number of cracks has an adverse effect on the value of both KU and CF, where for some cases the values are even less than that of the healthy case. The reason lies behind the parameters that these indicators depends on, such as the peak amplitude and average value.

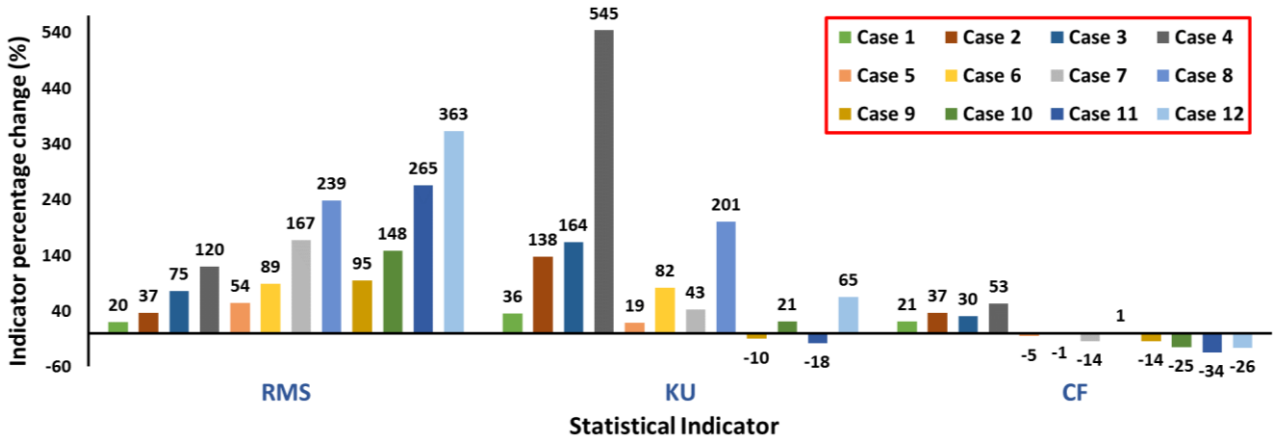

Figure 8: Performance of different time-domain indicators applied to the residual signal for the 12 cases

5. Vibration response in the frequency-domain

Several studies have found that the frequency-domain analysis is more sensitive to gear tooth cracks than the time-domain indicators [1]. The peak spectrum amplitude of the residual signal increases as the severity of faults increases, as well as the number of sidebands. Thus, the spectra of all the studied cases were obtained and analysed. A sample of the residual signal spectrum is shown in Fig. 9(a). The percentage change in the maximum peak of the residual signals spectra of the studied cases is depicted in Fig. 9(b). It can be seen that the peak amplitude increases dramatically as the number of cracks increases and as the CDP increases as well. However, there is a slight increase in the percentage change of the peak amplitude in the cases where the cracks coincide.

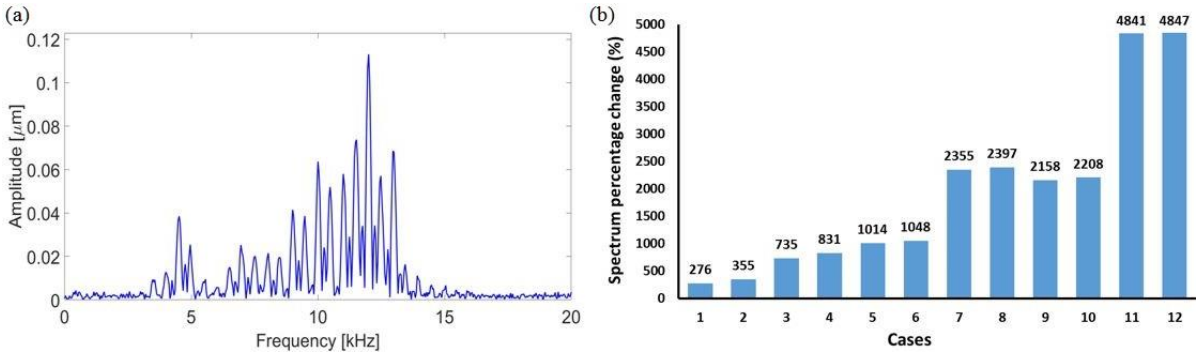

Figure 9: (a) Case 8 residual signal spectrum. (b) Percentage change in the residual signal spectrum peak.

6. Conclusions

This paper investigates the performance of some time-domain statistical indicators as well as the peak amplitude of the residual signal spectrum in the presence of multiple gear tooth cracks. In particular, the hunting tooth phenomenon was considered. From the simulation results, it was found that the GMS is severely affected by the mate of cracked teeth. Moreover, the amplitude of the time-domain signal almost doubles due to the hunting tooth phenomenon. The values of both the KU and RMS are higher when the cracks coincide. For the single crack cases, the KU is the most sensitive indicator, however, the RMS is the most sensitive in case of multiple cracks. The CF is the least sensitive to all the studied cases. The peak amplitude of the residual signal spectrum should be used for early detection of gear tooth cracks as the percentage change is substantially higher than that of the time-domain indicators.

REFERENCES

1. Mohammed OD, Rantatalo M, Aidanpää JO, Kumar U. Vibration signal analysis for gear fault diagnosis with various crack progression scenarios, *Mechanical Systems and Signal Processing*, **41** (1–2), 176-195, (2013).
2. Wang J. *Numerical and Experimental Analysis of Spur Gears in Mesh*, Master of Science Thesis, Curtin University of Technology, Perth, (2003).
3. Li CJ, Lee H. Gear fatigue crack prognosis using embedded model, gear dynamic model and fracture mechanics, *Mechanical Systems and Signal Processing*, **19** (4), 836–846, (2005).
4. Ma H, Zeng J, Feng R, Pang X, Wang Q, Wen B. Review on dynamics of cracked gear systems, *Engineering Failure Analysis*, **55,** 224–245, (2015).
5. Chen Z, Shao Y. Dynamic simulation of spur gear with tooth root crack propagating along tooth width and crack depth, *Engineering Failure Analysis*, **18** (8), 2149–2164, (2011).
6. Mohammed OD, Rantatalo M, Aidanpää JO. Improving mesh stiffness calculation of cracked gears for the purpose of vibration-based fault analysis, *Engineering Failure Analysis*, **34**, 235–251, (2013).
7. Chaari F, Fakhfakh T, Haddar M. Analytical modelling of spur gear tooth crack and influence on gearmesh stiffness, *European Journal of Mechanics - A/Solids*, **28** (3), 461–468, (2009).
8. Mohammed OD, Rantatalo M, Aidanpää J-O. Dynamic modelling of a one-stage spur gear system and vibration-based tooth crack detection analysis, *Mechanical Systems and Signal Processing*, **54–55**, 293–305, (2015).
9. Yu W, Shao Y, Mechefske CK. The effects of spur gear tooth spatial crack propagation on gear mesh stiffness, *Engineering Failure Analysis*, **54**, 103–119, (2015).
10. Howard I, Jia S, Wang J. The dynamic modelling of a spur gear in mesh including friction and a crack, *Mechanical Systems and Signal Processing*, **15** (5), 831–853, (2001).